Research Article

Ganoderma lucidum Extract as Corrosion Inhibitor for Carbon Steel in H$_2$SO$_4$

Ruben Suarez-Hernandez[1], Gloria Dominguez-Patiño[2], Isaac Tello[3], Jose Gonzalo Gonzalez-Rodriguez*[1]

[1]Universidad Autonoma del Estado de Morelos, CIICAp, AV. Universidad 1001, 62209-Cuernavaca, Mor., Mexico.
[2]Universidad Autonoma del Estado de Morelos, Fac. de Ciencias Biologicas, AV. Universidad 1001, 62209-Cuernavaca, Mor., Mexico
[3]Universidad Autonoma del Estado de Morelos, Centro de Estudios Bioticos , Av. Universidad 1001, 62209-Cuernavaca, Mor., Mexico

Abstract

The possibility of using *Ganoderma lucidum* extract as corrosion inhibitor for 1018 carbon steel in 0.5 M H$_2$SO$_4$ was evaluated by using potentiodynamic polarization curves and electrochemical impedance spectroscopy. The tests were supported by qualitative chemical tests, UV-Vis and FTIR spectroscopy. It was proved that *G. lucidum* is a good inhibitor, with its efficiency increasing with its concentration, reaching vales higher than 90%. In addition to the decrease in the corrosion current density, the passive current density was also decreased by forming a passive film containing iron oxide/hydroxide and proline present in the extract.

Keywords: Metals, FTIR, electrochemical impedance, corrosion.
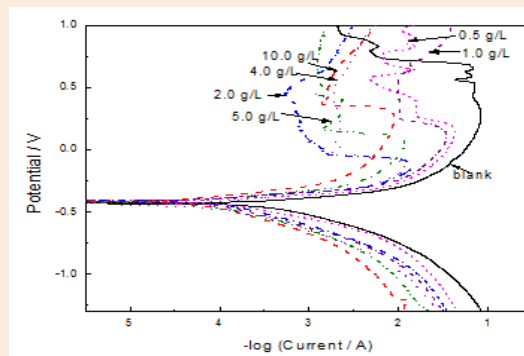
***Correspondence**
Jose Gonzalo Gonzalez-Rodriguez,
Email: ggonzalez@uaem.mx

Introduction

One of the most widely used methods to fight corrosion is the use of corrosion inhibitors. The known hazardous effects of most synthetic organic inhibitors and restrictive environmental regulations have compelled and motivated researchers to focus on the need to develop cheap, non-toxic and environmentally benign natural products such as leaves, fruits or seeds extracts, which can be used as corrosion inhibitors. It can be found in the literature a huge amount of research works related with the use of natural products extracts to be used as "green" corrosion inhibitors due to the presence of complex organic species such as tannins, alkaloids and nitrogen bases, carbohydrates and proteins as well as their acid hydrolysis products [1-20]. The use of these natural products they are more effective and highly environmentally benign compared to organic and inorganic inhibitors used in chemical or any industrial applications. Some of the natural products which have been proved to be good corrosion inhibitors are Aloe [2], *Coriandrum sativum* [3], *Green Bambusa Arundinacea* leaves [4], *Artemisia pallens* [5] and Gum Arabic [7] among others.

Among the plants with known antioxidant properties, *Ganoderma lucidum*, known as Ling Zhi in China and Reisshi in Japan has been shown to possess potent antioxidant activity in multiple research studies with little or no side effects [21-27]. In a human intervention study, ingestion of *G. lucidum* supplement was found to cause an acute increase in plasma antioxidant capacity [28]. *G. lucidum* polysaccharides have been proven to be the bioactive constituents responsible for many health benefits such as anticancer and immune-stimulatory effects with antioxidant activity [28]. It is usually used in infusions of carpophores for improving health and longevity and for preventing and/or treating hepatitis, chronic, gastritis, tumor growth and immunological troubles. *G. lucidum* contains two

relevant groups of compounds, triterpenes and polysaccharides, together with proteins, steroids, lectins and adenosine analogues [29, 30]. Among its demonstrated pharmaceutical properties, ganoderma´s anticancer, inmunomodulatory, hypoglycaemic, hypolipidemic and hepatoprotective properties stand out. Various pharmacological studies have demonstrated the plant´s anticancer properties and its triterpene content, while its immunological properties have generally been associated with its polysaccharide components [31, 32]. Several clinical trials have also shown the potential usefulness of G. *lucidum* as immunostimulant in patients undergoing chemotherapy or anticancer drug treatment [33]. Thus, since *G. lucidum* has several components with antioxidant properties, the goal of this paper is to evaluate its use as a corrosion inhibitor for carbon steel in 0.5 M H_2SO_4.

Experimental procedure

Material tested in this work was 1018 carbon steel containg 0.14%C, 0.90% Mn, 0.30%S, 0.030% P and as balance Fe, encapsulated in commercial epoxic resin with an exposed area of 1.0 cm^2. The aggressive solution, 0.5 M H_2SO_4 was prepared by dilution of analytical grade chemical in distilled water. G. *lucidum* was grown and provided by the Faculty of Agrosciences in our university. For the extraction, dried G. *lucidum* was soaked in 2/3 ethanol+1/3 water during 21 days obtaining a solid, wich was weighted and dissolved in ethanol and used as a stock solution and used then for preparation of the desired concentrations by dilution. Used concentrations included 0, 0.5, 1, 2, 4, 5 and 10 g/L. The IR spectra were recorded with KBr pellets on a Tensor 27 Bruker spectrophotometer between 400 and 4000 cm^{-1} whereas UV-Vis analysis was done by using a Uv-Vis 8453 Agilent spectrophotometer. To identify reducing sugars the "Fehling's Test" was used while forming Cu_2O in solution. In this process, Cu^{2+} ions are reduced to Cu^+ by reducing sugars upon heating in an alkaline medium in the presence of tartrate to precipitate brick red or yellow Cu_2O crystals. Two drops of Fehling's A ($CuSO_4.5H_2O$) and B (Sodium tartrate + NaOH) solution were added to 0.5 g of the extract. Estimation of amino acids was done by the ninhydrin reaction which is based in the reaction of ninhydrin with primary amino groups to form the purple dye now called Ruhemann's purple.

Electrochemical techniques employed included potentiodynamic polarization curves and electrochemical impedance spectroscopy measurements, EIS. In all experiments, the carbon steel electrode was allowed to reach a stable open circuit potential value, E_{corr}. Polarization curves were recorded at a constant sweep rate of 1 mV/s at the interval from -1000 to +1000 mV respect to the E_{corr} value. Measurements were obtained by using a conventional three electrodes glass cell with two graphite electrodes symmetrically distributed and a saturated calomel electrode (SCE) as reference. Corrosion current density values, I_{corr}, were obtained by using Tafel extrapolation. Electrochemical impedance spectroscopy tests were carried out at E_{corr} by using a signal with amplitude of 10 mV in a frequency interval of 100 mHz-20 KHz. An ACM potentiostat controlled by a desk top computer was used for the polarization curves, whereas for the EIS measurements, a model PC4 300 Gamry potentiostat was used.

Results and discussion

The polarization curves for carbon steel in 0.5 M H_2SO_4 with the addition of different *G. lucidum* concentrations are shown in **Figure 1**. This figure shows that in th blank, uninhibited solution, the steel displays an active passive behavior with an E_{corr} value close to -430 mV and a corrosion current density value around 0.3 mA/cm^2. As the potential is made more anodic, the current density starts to increase reaching a steady state value, or passive region, around a pasivation potential value, E_{pas}, close to 250 mV where the current density remains more or less constant reaching a passive current density value, I_{pas}, around 63 mA/cm^2. As the potential is made more anodic up to 580 mV the anodic surrent density decreases down to 1 mA/cm^2 forming what looks like a second passive region. As soon as the inhibitor is added, the anodic current density decreases and the passive region is formed at lower anodic potentials. The E_{corr} value remained virtually the same regardless of the inhibitor concentration, but the corrosion current density decreases as the inhibitor concentration decreases down to one order of magnitude reaching the lowest value when10 g/L of inhibitor are added. Even more, both the E_{pas} and I_{pas} values decrease as the inhibitor concentration increases, reaaching the lowest value with 2.0 g/L where the I_{pas} value is lowered for almost two orders

of magnitude. However, with a further increase in the inhibitor concentration both values increase once again, being in all cases lower than that value for the uninhibited solution.
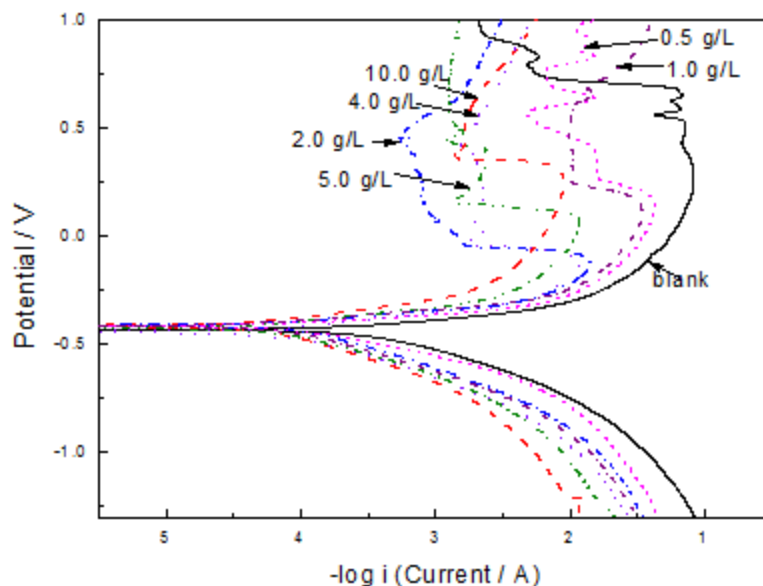

Figure 1 Effect of *G. lucidum* concentration in the polarization curves for carbon steel in 0.5 M H_2SO_4 at 25 ^{0}C.

Table 1 Electrochemmical parameters obtained from the polarization curves

C_{inh},	$-E_{corr}$,	I_{corr},	E_{pas},	I_{pas},	I.E.,	β_a	β_c
g L^{-1}	mV	A	mV	A	%	mV dec^{-1}	mV dec^{-1}
0	430	3×10^{-1}	230	63	----	152	198
0.5	410	8×10^{-2}	250	10	73	50	188
1.0	413	6.5×10^{-2}	270	9	78	60	186
2.0	445	5×10^{-2}	370	0.5	83	78	195
4.0	410	4×10^{-2}	-35	2.0	86	55	185
5.0	415	4×10^{-2}	170	1.4	86	60	195
10.0	412	1×10^{-2}	-40	1.7	95	45	200

Table 1 gives a summary of the electrochemical parameters obtained from these polarization curves. In this table, inhibitor efficiency (I.E.%) was calculated by using the following equation:

$$I.E. \ (\%) = \frac{I_{corr} - I_{corr(inh)}}{I_{corr}} \ x \ 100 \qquad [1]$$

Where, I_{corr} and $I_{corr(inh)}$ are the corrosion current density values in absence and presence of inhibitor respectvely. This table shows that the inhibitor efficiency value increases with an increase in the inhibitor concentration reaching a value around 95% when 10 g/L of *G. lucidum* are added. In addition to this, it can be seen that tha cathodic Tafle

slope remained virtually the same regardless of the inhibitor concentration, but the anodic slope was decreased as soon as the inhibitor was added to the solution, indicating that *G. lucidum* acts as an anodic type of inhibitor. *G. lucidum* has been shown to possess potent antioxidant activity in multiple research studies with little or no side effects [24, 27]. This activity is shown in its ability to form very protective passive film on 1018 carbon steel exposed to 0.5 M H_2SO_4 solution with an I_{pas} value 100 times lower than that formed in absence of *G. lucidum*.

In order to evaluate the adsorption process of *G. lucidum* on the 1018 carbon steel surface, Langmuir, Temkin and Frumkin adsorption isotherms were obtained according to the following equations:

$$\text{Langmuir: } \theta/1\text{-}\theta = KC_{inh} \hspace{3cm} [2]$$

$$\text{Temkin: } \log(\theta/C_{inh}) = \log K - g\theta \hspace{2.5cm} [3]$$

$$\text{Frumkin: } \log (\theta C_{inh})/(1\text{-}\theta) = \log K + g\theta \hspace{2cm} [4]$$

Where, θ is the surface coverage, K is the adsorption-desorption equilibrium constant, C_{inh} is the inhibitor concentration and g is the adsorbate interaction parameter. **Figure 2** indicates that *G. lucidum* adsorbed onto the carbon steel surface following a Frumkin adsorption isotherm since it had an R^2 value of which is very close to the unit
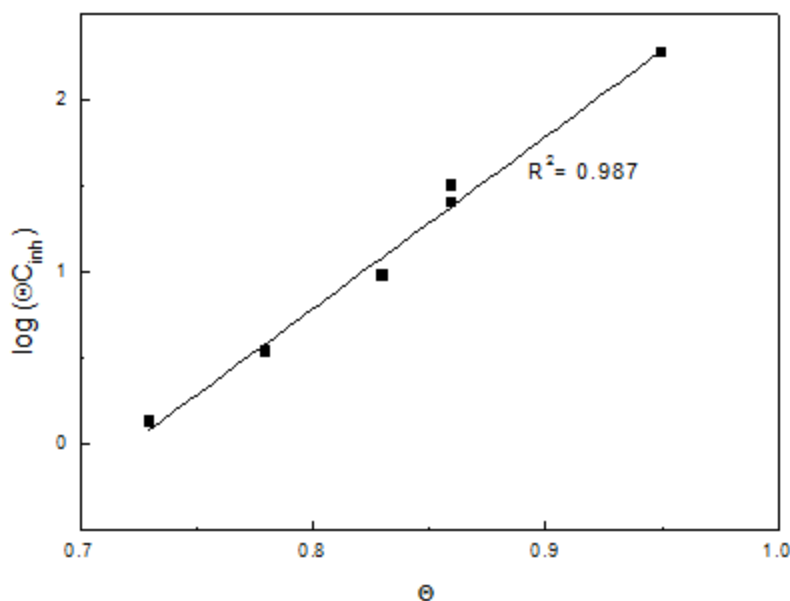

Figure 2 Frumkin adsorption isotherm for G. lucidum on carbon steel immersed in 0.5 M H_2SO_4 at 25 ^{0}C

The effect of *G. lucidum* concentration in the Nyquist diagrams for 1018 carbon steel in 0.5 M H_2SO_4 is shown in **Figure 3** a where it can be seen that data describe a single, depressed, capacitive-like semicircle at all frequency values, indicating a corrosion proccess controlled by charge transfer crom the metal to the electrolyte through the double electrochemical layer. As soon as the inhibitor is added, the semicircle diameter increases and keeps increasing with a further increase in its concentration reaching its highest value with the addition of 10 g/L of *G. lucidum*. The shape is maintained throughout the whole test period, indicating that almost no change in the corrosion mechanism occurred due to the change in the inhibitor concentration. When Nyquist plot contains a "depressed semicircle with the centre under the real axis", such behavior is characteristic for solid electrodes and often referred to as frequency dispersion which has been attributed to the surface heterogeneity due to surface roughness, impurities or dislocations [34], fractal structures [35], distribution of activity centers, inhibitors adsorption and formation of porous layers [36].

Bode diagrams in both modulus and phase angle formats are shown in **Figure 3 b**. For the blank, uninhibited solution, the modulus was the lowest and it starts to increase as the frequency increases up to 10 Hz, where it reaches a steady state value until a frequency value around to 0.1 Hz, where its value starts to decrease, indicating an increase in the corrosion rate. As soon as the inhibitor is added, the modulus increases in value as the inhibitor concentration is increased, reaching its highest value with the addition of 10 g/L of *G. lucidum*. Phase angle shows only one peak around 100 Hz for the uninhibited solution, and it shifts towards lower frequency values as the inhibitor concentration is increased.
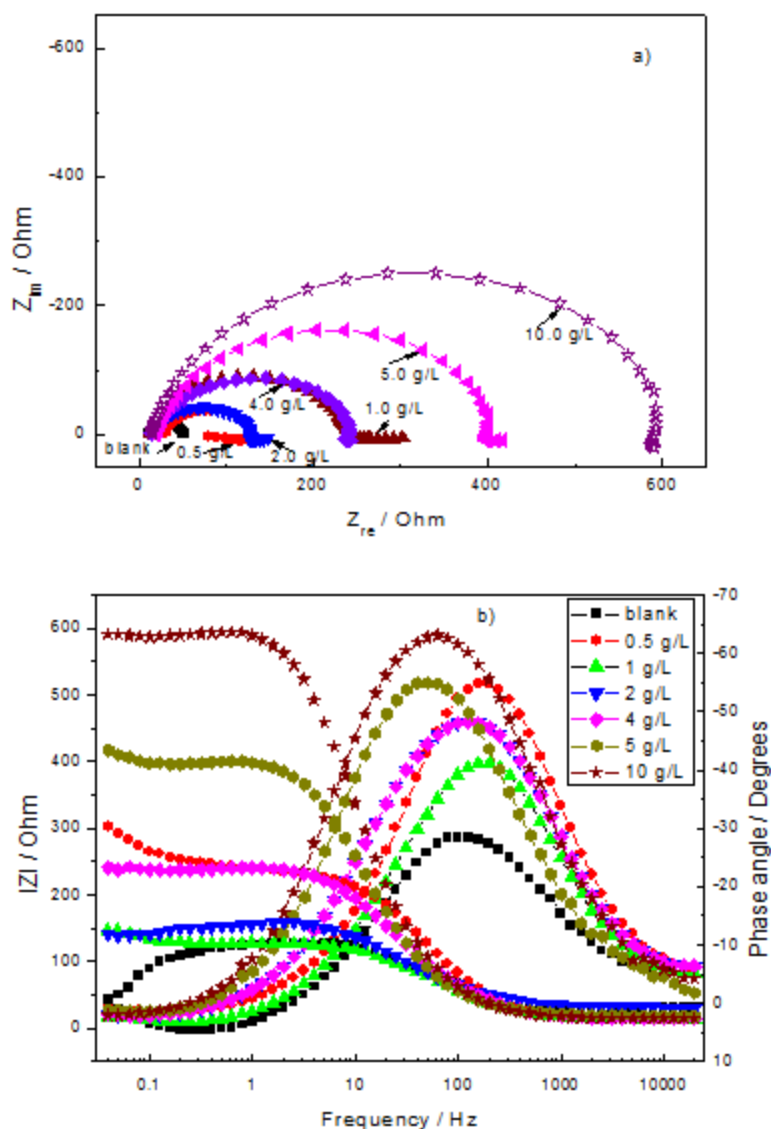

Figure 3 Effect of *G. lucidum* concentration in the a) Nyquist and b) Bode diagrams for carbon steel exposed to 0.5 M H_2SO_4 at 25 ^{0}C.

The various impedance parameters such as charge transfer resistance (R_{ct}), C_{dl}, n, and g (%) calculated are depicted in Table 2. The value of ''n'' seems to be associated with the non-uniform distribution of current as a result of roughness and possible oxide surface defects. When n = 1, CPE is an ideal capacitor. A true capacitive behavior is rarely obtained. The ''n'' values close to 1(**Table 2**) represent the deviation from the ideal capacitor. A constant phase element (CPE) is utilized for data fitting instead of an ideal capacitor, since the ''n'' values obtained were in

the range of 0.9, the value obtained from the data fitting was taken as the capacitance. Inhibitor efficiency values (I.E. %) were calculated by using the following equation:

$$IE\ (\%) = \frac{R_{ct\ (inh)} - R_{ct}}{R_{ct\ (inh)}} \times 100 \qquad\qquad [5]$$

Where, R_{ct} and $R_{ct(inh)}$ are charge transfer resistances in the absence and in the presence of inhibitor, respectively.

Table 2 Impedance parameters and inhibitor efficiency values for carbon steel after immersion in 0.5 M H_2SO_4 containing different concentrations of *G. lucidum* at 25 ^{0}C

C_{inh}, g L^{-1}	R_s, Ohm	R_{ct}, Ohm	C_{dl}, F cm^{-2}	n	I.E., %
0	10	52	5.3 x 10^{-5}	0.88	------
0.5	29	120	3.2 x 10^{-5}	0.87	56
1.0	13	302	2.6 x 10^{-5}	0.96	82
2.0	14	132	1.5 x 10^{-5}	0.87	60
4.0	14	241	3.3 x 10^{-5}	0.85	78
5.0	18	416	3.9 x 10^{-5}	0.86	88
10.0	14	592	4.2 x 10^{-5}	0.88	91

The inhibition efficiency values, calculated from a.c. impedance measurements, show the same trend as those obtained from polarization studies previously described (**Tables 1 and 2**). From **Table 2**, it is observed that addition of inhibitors increases R_{ct} values (52–592 Ohm cm^2) when the inhibitor concentration increases up to 10 g/L; a decreases in the double layer capacitance value (400–160 mF cm^2) is obtained when the inhibitor concentration increases up to 2.0 g/L which indicated reduction in corrosion rate, but a decrease in the C_{dl} value is observed with a further increase in the inhibitor concentration. The decrease in C_{dl} can be interpreted as due to the adsorption [37], of the crude extract on the mild steel surface. Double layer formed at the electrode–solution interface is considered as an electric capacitor, whose capacitance decreases due to the displacement of water molecules and other ions originally adsorbed on the electrode by the crude methanolic extract molecules, forming a protective film.

It is generally accepted that the first step during the adsorption of an organic inhibitor on a metal surface usually involves replacement of water molecules absorbed on the metal surface:

$$Inh_{sol} + xH_2O_{ads} \rightarrow Inh_{ads} + xH_2O_{sol} \qquad\qquad [6]$$
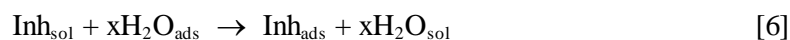
The inhibitor may then combine with freshly generated Fe^{2+} ions on steel surface, forming metal-inhibitor complexes [25, 26]:

$$Fe \rightarrow Fe^{2+} + 2e \qquad\qquad [7]$$

$$Fe^{2+} + Inh_{ads} \rightarrow [Fe\text{-}Inh]_{ads}^{2+} \qquad\qquad [8]$$
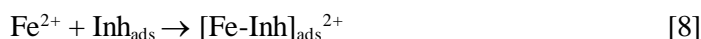
The resulting complex, depending on its relative solubility, can either inhibit or catalyze further metal dissolution or increase its corrosion rate. At low concentrations the amount of *G. lucidum* is insufficient to form a compact complex with the metal ions, so that the resulting adsorbed intermediate will be readily soluble in the acidic environment. But at relatively higher concentrations more *G. lucidum* molecules become available for complex formation, which subsequently diminishes the solubility of the surface layer, leading to improve the inhibition of metal corrosion.
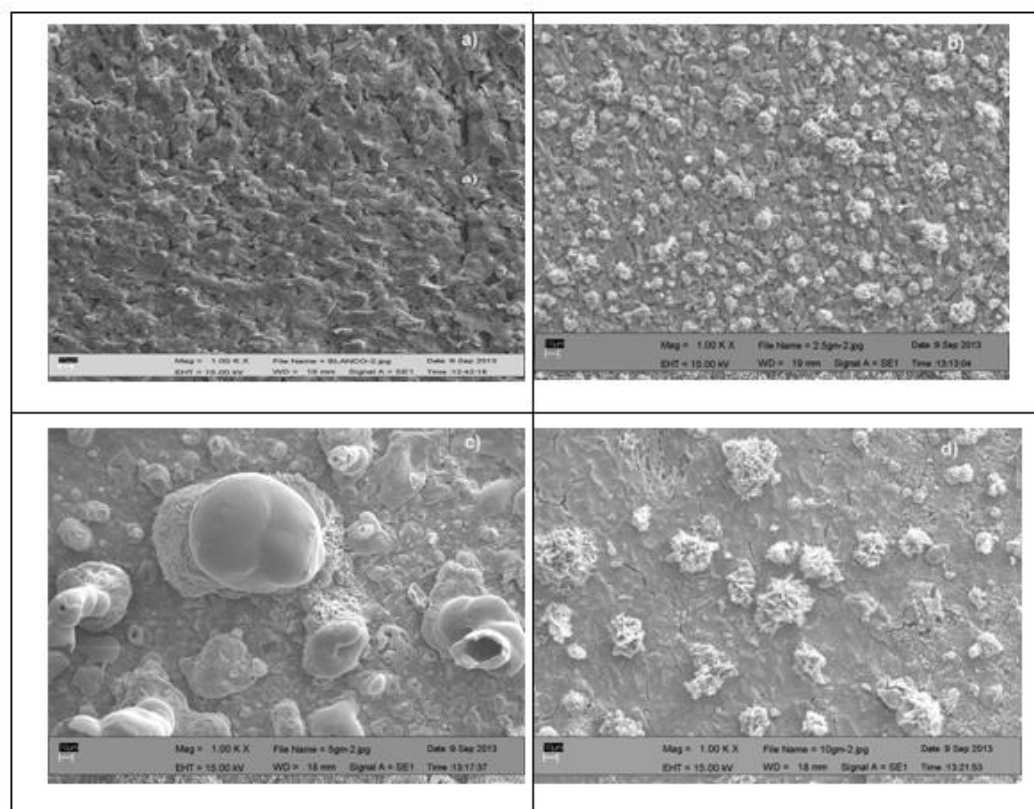
Figure 4 SEM micrographs of carbon steel after 24 hours of exposure to 0.5 M H_2SO_4 in presence of a) 0, b) 2.0, c) 5.0 and e) 10.0 g/L of *G. lucidum*.
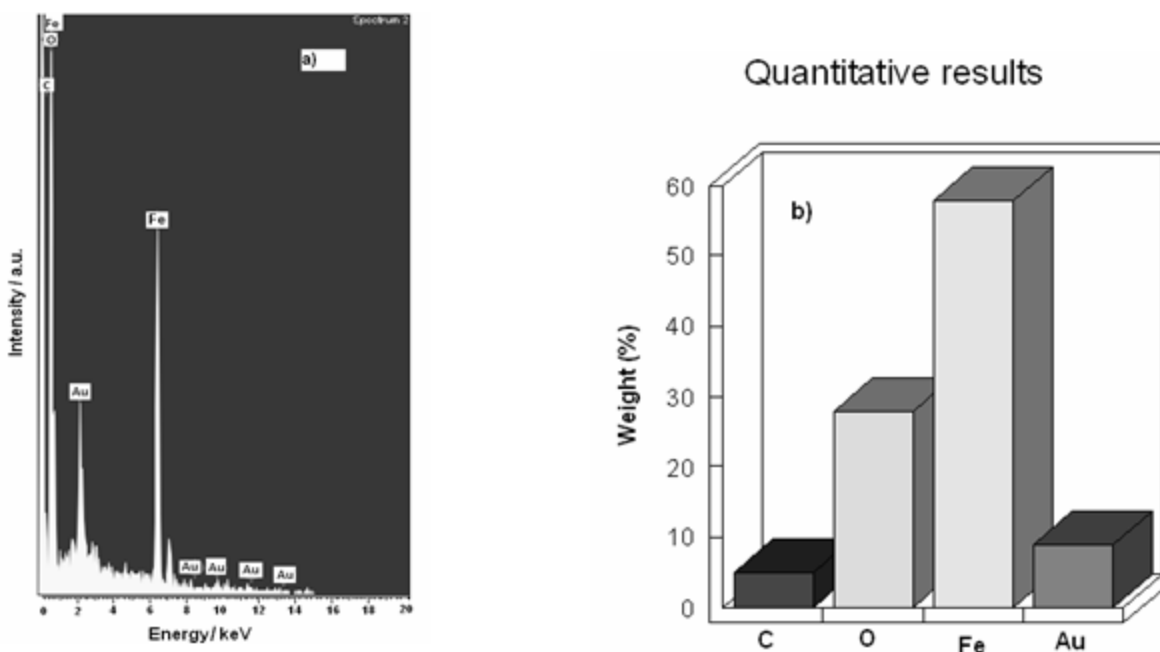

Figure 5 Microchemical analysis of corroded carbon steel exposed to 0.5 M H_2SO_4 + 2.0 g/L of *G. lucidum* at 25 ^{0}C showing in a) EDX analysis and in b) semi-quantitative results.

To establish whether inhibition is due to the formation of an organic film on the metal surface, scanning electron micrographs were taken. **Figure 4** shows the SEM micrograph of the carbon steel surface after of the immersion in 0.5 M H_2SO_4 with and without corrosion inhibitor where it can be seen that the steel exposed to the solution without inhibitor forms a porous layer full of micro cracks, **Figure 4 a**. The aggressive solution can penetrate through these defects and corrode the underlying metal. However, in presence of inhibitor the surface has remarkably improved with respect to its smoothness, less porous and micro cracks, indicating considerable reduction of corrosion rate. This improvement in surface morphology is due to the formation of a good protective film on carbon steel surface which is responsible for inhibition of corrosion. Indeed, these pictures show that *G. lucidum* has a strong tendency to adhere to the steel surface and can be regarded as good inhibitor for steel corrosion in normal sulfuric medium. Microanalysis done on the surface of the metal exposed to 0.5 M H_2SO_4+ 2.0 g/L of inhibitor, **Figure 5**, shows the presence of C, O, Fe and Au, suggesting the formation of a compound including iron oxide/hidroxide and C. The former comes from the use of Au for the preparation nof specimens to be seen in the SEM.

Table 3 Bands assignation to the *G. lucidum* FTIR spectrum

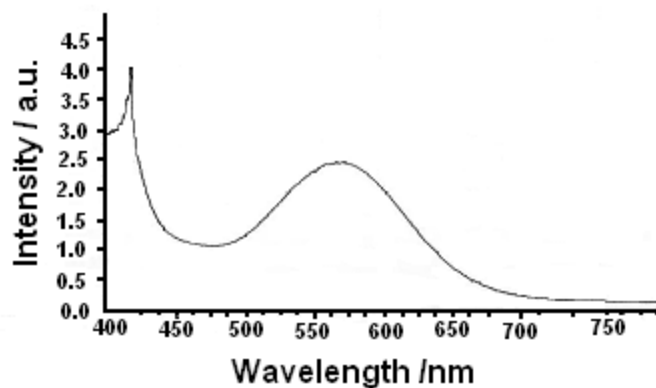| Wavenumber cm⁻	Functional group	Vibration type	Range cm⁻¹
3000	C -H	Stretching	2800-300
2032	C=NH	Stretching	1500-2000
1637	C=O	Stretching	1690-1720
1384	(-CH₃)	Bending	1375-1380
1200	C-OH	Bending	1200-1500
1056	(=C-H)	Bending	1000-650
866	(=C-H)	Bending	1000-650
3480	OH	Strectching	3200-3400
600	(=C-H)	Bending	1000-650

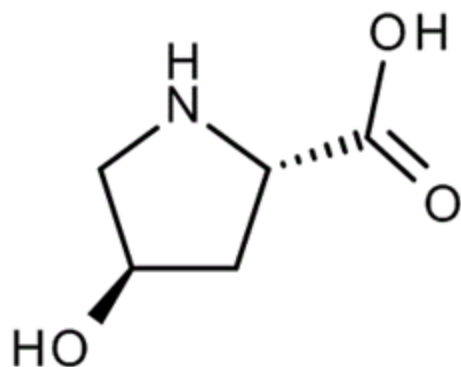**Figure 6** UV-Vis spectrum for pure ethanolic *G. lucidum* extract
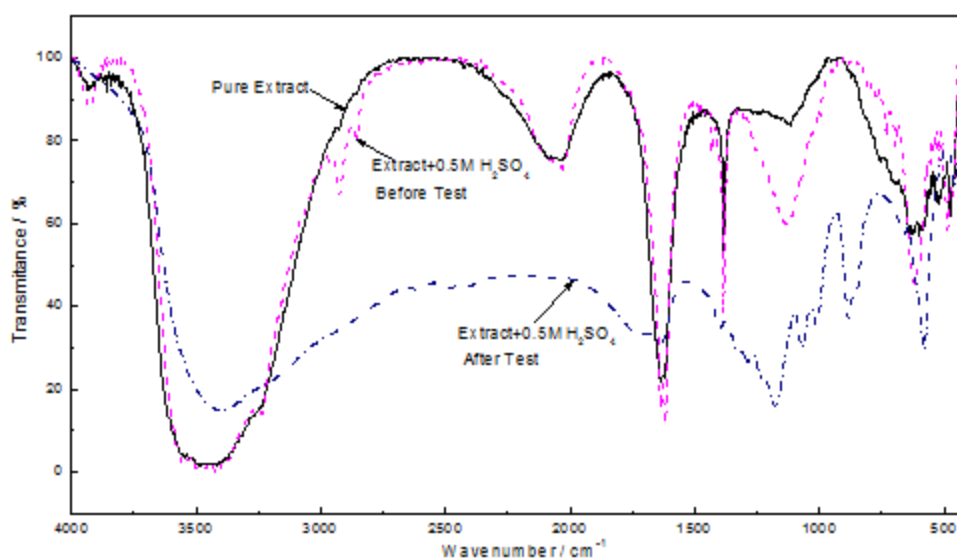
Figure 7 Molecular structure of proline.

Figure 8 FTIR spectra for *G. lucidum* pure extract and G. lucidum+0.5 M H_2SO_4 before and after corrosion test.

G. lucidum and its polysaccharide, polysaccharide-protein, and phenolic constituents were reported to possess antioxidant activity, to inhibit lipid peroxidation, and to scavenge free radicals [28] . By using Fehling's Test, it was observed the precipitatation of brick red Cu_2O crystals, indicating the presence of reducing carbohydrates. Similarly, Ninhydrin Reaction of the extract produced a purple dye indicating the presence of primary amino acids in the extract. UV-Vis diagram shown in **Figure 6** indicates the presence of this compound at 450 and 750 nm, together with proline, a secondary amino acid, at 416 nm, with a molecular structure as given in **Figure 7**. FTIR spectra of the crude ethanolic extract, extract + 0.5 M H_2SO_4 before and after the corrosion test are shown in **Figure 8** whereas identified functional groups are given in **Table 3**. Broad bands in the range of 3000–3600 cm^{-1} can be assigned to the OH stretching vibrations of the crude ethanolic extract, whereas the peak at 2032 cm^{-1} corresponds to imino HN=C bonds, presents in a secondary amino acid; the peak around 1637 cm^{-1} corresponds to cetone C=O bonds from the the reducing carbohydrates; the peak around 1175 cm^{-1} corresponds to C-N bonds, from the amino acids. Once the extract has been added to the acid a decrease in the peak at 1384 cm^{-1} corresponding to -CH$_3$ and an increase in the peak at 3250 cm^{-1}, corresponding to the OH bond stretching can be observed. After the corrosion test, a decrease in the C=O peak together with the signal at 3500 cm^{-1}, corresponding to the OH band, can be observed, maybe due to the formation of FeOH, and a broadening of a band in the 2500-300 cm^{-1} interval. The presence of Fe and O on the

protective film was shown in **Figure 5**, which supports the idea of the formation of FeOH in the passive film for the prevention of corrosion. The high inhibitive performance of this mushroom extract suggests a strong bonding of the *G. lucidum* derivatives on the metal surface due to presence of lone pairs from heteroatom (oxygen) and p-orbitals, blocking the active sites and therefore decreasing the corrosion rate. Therefore, bonding between inhibitor molecules onto carbon steel surface occurs through sharing electrons of the OH group present in proline molecule of the pure extract and vacant d-orbitals of iron according to eqs.6-8 and following a Frumkin adsorption isotherm.

Conclusion

G. lucidum has been proved to be an efficient inhibitor in the corrosion of carbon steel in 0.5 M H_2SO_4. Inhibition efficiency increased with the *G. lucidum* concentration reaching values higher than 90% with 10.0 g/L. However, the passivation current density was decreased two orders of magnitude by using 2.0 g/L of *G. lucidum*. Nyquist diagrams showed that the charge transfer resistance increased with increasing the *G. lucidum* extract. The adsorption of the inhibitor molecules on to carbon steel obeyed a Frumkin adsorption isotherm forming a pasiivating film. This passive film, an Fe-inhibitor comoplex, contained proline, and probably iron oxide/hydroxide.

References

[1]   Vasconcelos-Torres V, Salgado-Amado R, Faia de Sá C, Lopez-Fernandez T, Alberto da Silva Riehl C, Guedes-Torres A, D'Elia E, Corr Sci 2011, 53, 2385-2395.
[2]   Fares M M, Maayta AK, Al-Qudah M M, Corr Sci 2012, 60, 112-124.
[3]   Torres VV, Rayol VA, Magalhães M, Viana GM, Aguiar LCS, Machado S P, Orofino H, D'Elia E, Corr Sci 2014, 79, 108-120.
[4]   Halambek J, Berkovic K, Vorkapic-Furac J, Mat Chem Phys 2013, 137, 788-801.
[5]   El Bribri A, Tabyaoui M, Tabyaoui B, El Attari H, Bentiss F, Mat Chem Phys 2013, 141, 240-252.
[6]   Chauhan LR, Gunasekaran G, Corr Sci 2007**,** 49, 1143-1155.
[7]   Okafor P C, Ikpi M E, Uwah IE, Ebenso EE, Ekpe UJ, Umoren SA, Corr Sci 2008, 50, 2310-2323.
[8]   Ashassi-Sorkhabi H, Asghari E, J Appl Electrochem 2010, 40, 631-640.
[9]   Quraishi MA, Singh A, Singh VK, Yadav D K, Singh AK, Mat Chem Phys 2010, 122, 114-121.
[10] El-Etre AY, Mat Chem Phys 2008, 108, 278-291.
[11] Avwiri G O, Igho FO, Materials Letters 2003, 57, 3705-3709.
[12] Obot IB, Obi-Egbedi NO, J Appl Electrochem 2010, 40, 977-985.
[13] Rahim A A, Rocca E, Steinmetz J, Kassim M J, Adnan R, Sani Ibrahim M, Corr Sci 2007, 49, 402-418.
[14] Lowmunkhong P, Ungthararak D, Sutthivaiyakit P, Corr Sci 2010, 52, 30-42.
[15] Olusegun K, Abiola JOE, Otaigbe OJ, Corr Sci 2009, 5, 18791894.
[16] Khaled K F, Mat Chem Phys 2008, 112, 104-111.
[17] De Souza F S, Spinelli A, Corr Sci 2009, 51, 642-656.
[18] Loto CA, Lotto R T, Popoola API, Int J Electrochem Sci 2011, 6, 3452-3465.
[19] Valek L, Martinez S, Materials Letters 2007, 61, 148-152.
[20] Oguzie EE, Corr Sci 2007, 49, 1527-1539.
[21] Bentiss F, Lagrence M, Traisnel M, Corrosion 2000, 56, 733-742.
[22] Rzedowski J, Calderon G (Ed), Chapter II, Flora del Bajio y de Regiones Adyacentes, Ocampo AG, Grijalvo Editors, Mexico, 2003, p. 1-7.
[23] Houghton PJ, J Ethnopharmacy 1984, 11, 293-305.
[24] Yen G C, Wu J Y, Food Chemistry 1999, 65, 375-384.
[25] Aruoma O I, Food Chemistry and Toxicology 1994**,** 32, 4671-4683.
[26] Halliwell B, Aeschbach R, Loliger J, Food Chemistry and Toxicology 1995, 33, 601-610.
[27] Mau J L, Lin H C, Chen C C, J Agriculture and Food Chemistry 2002, 50, 6072-6073.
[28] Wachtel-Galor S, Szeto Y T, Tomlinson B, Int J Food Science and Nutrition 2004, 55, 75-83.
[29] Wachtel-Galor S, Tomilson B, Benzoe IFF, British Journal of Nutrition 2004, 91, 263-272.

[30] Xu J, Liu W, Yao W, Pang X, Yin D, Gao X, Carbohydrate Polymers 2009, 78, 227-235.

[31] Lin ZB, J Pharmacology Science 2005, 99, 144-152.

[32] Fan L, Li J, Deng K, Ai L, Carbohydrate Polymers 2012, 87, 1849-1861.

[33] X.L. Xhu, A.F. Chen, Z.B. Lin, J. Ethnopharmacology, 2007, 111, 219.

[34] Stoynov ZB, Grafov BM, Savova-Stoynova B, Elkin VV, Electrochemical Impedance, 1991,Nauka, Moscow,.

[35] Mulder WH, Sluyters JH, Electrochimica Acta 1988, 33, 303-312.

[36] Hermas AA, Morad MS, Wahdan MH, J App Electrochem, 2004, 34, 95-107.

[37] Bentiss F, Gassama D, Barbry L, Gengembre H, Vezin M, Lagrenee-Traisnel M, Appl Surf Sci 2006, 252, 2684- 2696